ARTICLE IN PRESS

Algal Research xxx (xxxx) xxx–xxx

Contents lists available at ScienceDirect

Algal Research

journal homepage: www.elsevier.com/locate/algal

# A comparison of spectral macroalgae taxa separability methods using an extensive spectral library

Y. Chao Rodríguez[a,*], J.A. Domínguez Gómez[a], N. Sánchez-Carnero[b,c], D. Rodríguez-Pérez[a]

[a] Departamento de Física Matemática y de Fluidos, Facultad de Ciencias, Universidad Nacional de Educación a Distancia (UNED), Spain
[b] Grupo de Oceanografía Física, Universidad de Vigo, Spain
[c] Centro Para el Estudio de Sistemas Marinos (CESIMAR), Centro Nacional Patagónico, Argentina

ARTICLE INFO

*Keywords:*
Algae species
Spectral classification
Spectral library
Colorimetry
Photosynthetic pigments
True Skill Statistics (TSS)

ABSTRACT

Remote sensing is one the most promising approaches to coastal area cartography, including mapping algae forests. After discrimination of algal communities from other benthic habitats, next step is species discrimination (from other algae). Spectral signature provides the most complete remote description to characterize any algae. In this work spectral signatures are studied from the point of view of taxa separability to assess the potential use of remote sensors to map seaweed in coastal waters. Three approaches were tested: Red-Green-Brown colorimetry (sRGB), optimal spectral boundary separation based on True Skill Statistics (TSS-OB), and pigment absorbance band detection by Derivative Spectroscopy (DS). An extensive spectral library of 36 algal species present in the Atlantic Galician coast (NW of Spain) is used to test and validate these methods. The results show that the three broad taxa of red, green and brown algae can be separated by all three methods (Cohen's kappa of 0.697, 0.891 and 0.910, respectively). The TSS-OB and the DS approaches provide almost perfect classification (despite some anomalous specimens), with DS being slightly better. The sRGB approach, useful for in situ photographic classification, also provides good results.

## 1. Introduction

Submerged vegetation, seagrass and macroalgal communities, play an ecologically important functional role in coastal ecosystems as they serve as habitats [1–3], mating and nursery grounds [4,5], feeding areas [6,7], and refuge [8,9] for many species. Moreover, they have an important contribution to primary production [10], sediment stabilization and coastline protection [11]. Despite their ecological importance, in recent years a decrease in the extension of these communities has been observed, and although many studies have addressed this problem [12–16] the causes of this degradation are not yet known.

Since the 1980's these studies have taken advantage of remote sensing because of its large coverage, periodicity, multispectral information (including non-visible regions of the spectrum) and low relative cost (in €/km$^2$) compared with on field surveys. These capabilities allow researchers to monitor large areas [17] repeatedly, studying the distribution and dynamics of macroalgae forests with reduced costs and sampling time [18–26].

One of the most important challenges in these works has been to distinguish algae from other substrates (underwater or emerged; [27]); shallow water models show that up to 19 m of very clean sea water these differences can be appreciated in the visible range [28], although this limit can be much smaller depending on water conditions. One step further is to classify different algae groups apart (or even species), for example, to monitor retreat of an indigenous algal species often associated with the spreading of an alien one [29,30]. This goal can be addressed because of the capability to detect algal optical properties, that is the absorption (by pigments) and reflection (by tissular structures) of light, from remote sensing images. Pigments of each phylum (and species), together with tissular morphology and cellular architecture, shape the spectral signature of each algae (the value of the spectral reflectance for each wavelength in the optical range). These optical properties are directly related to the biophysical characteristics that are used to perform algae classification in three different phyla (Table 1), following Lee [31]:

i.) The phylum Rhodophyta, also called “red algae”, is composed by a large assemblage of between 2500 and 6000 species [32]. Their characteristic pigments are chlorophyll *a* (Chl-*a*) and *d*, carotenoids and phycobiliproteins (mainly phycocyanin and phycoerythrin); the latter being responsible for their red color.
ii.) The phylum Clorophyta, also called “green algae”, are primarily

* Corresponding author.
*E-mail address:* ychao@dfmf.uned.es (Y. Chao Rodríguez).

http://dx.doi.org/10.1016/j.algal.2017.04.021
Received 22 September 2016; Received in revised form 19 April 2017; Accepted 21 April 2017


Please cite this article as: Chao Rodríguez, Y., Algal Research (2017), http://dx.doi.org/10.1016/j.algal.2017.04.021

**Table 1**
Macroalgae biophysical features.

| | Rhodophyta (red algae) | Clorophyta (green algae) | Heterokontophyta (brown algae) |
|---|---|---|---|
| Chl-*a* | X | X | X |
| Chl-*b* | – | X | – |
| Chl-*c*1 | – | – | X |
| Chl-*c*2 | – | – | X |
| Chl-*d* | X | – | – |
| Carotenoids | X | X (lutein) | X (fucoxanthin) |
| Phycocyanin | X | – | – |
| Phycoerythrin | X | – | – |

freshwater algae; only about 10% of them are marine [33]. Their characteristic pigments are similar to those of higher plants: Chl-*a* and Chl-*b*, cause of their common green color, and carotenoids (mainly lutein).

iii.) The phylum Heterokontophyta, specifically the family Phaeophyceae or "brown algae", contains the species of largest algae, including kelp that form forests such as *Sargassum muticum*, *Macrocystis* spp., etc. They derive their characteristic color from the large amounts of the carotenoid fucoxanthin as well as from any phaeophycean tannins that might be present. They have also Chl-*a*, and chlorophylls *c*1, and *c*2.

All these pigments shape the spectral signature of each alga. The more similar two species are (due mostly to their pigment contents), the more similar are their signatures. In this sense, having a complete spectral library can drastically help remote sensing classification [34] or assessment of biophysical conditions [35]. Optical remote sensing is based on sampling of spectral signatures at small windows (bands). If we know in detail the reflectance spectrum of a species of interest, we can simulate how it would appear when observed through the water column, and compare this with the remote sensing reflectance spectrum; optimization algorithms can also derive water column properties from this comparison [36].

Other authors, not focused on cartography, have also pointed out that having an extensive spectral library would help overcome limitations associated to multispectral remote sensing such as the need for extensive collection of in situ data to calibrate sensor dependent spectral response, or depth-dependent water column correction [37]. Despite these applications, macroalgae libraries in the literature are scarce and incomplete because of the cost of measurement processes and the lack of interested industries (contrary to minerals, for example). Some examples of algae libraries can be found in Kutser et al. [39,49], Vahtmäe et al. [41], Thorhaug et al. [42], Pu et al. [43], García et al. [44].

Different remote sensing approaches of algae classification have been used both with multispectral [45] or hyperspectral [46,47] satellite sensors. Remote sensing classification methods highlight distinctive spectral features, either in pre-selected bands (e.g., from a multispectral sensor) or in ad hoc bands, best adapted to the purposes of a study. For classifications based on spectral libraries, characteristic features are often assessed from the in-air spectra, considering optimal viewing conditions without the water column attenuating some of them (that is, classification of submerged vegetation will be worse than the best in-air classification). Among the approaches already published we will focus on the following:

**RGB-colorimetry**: As can be inferred from phyla classification, a major taxonomic feature of macrophytes is their visual color, or otherwise RGB components determined from their reflectance spectra. This simple and cheap approach (as only a digital camera is needed) has already been proposed to quantitatively describe seawater color [48] and assess biochemical properties of living organisms: microalgae [49], and corals [50].

**True Skill Statistics Optimal Band (TSS-OB)**: Kotta et al. [37] presented a method to separate taxa from their in-air spectra taking into account the statistical distribution of algae spectra in a library. From standardized spectra True Skill Statistics (TSS) [51] is computed to determine the optimal boundaries between spectral reflectances that best separate every pair of different phyla, thus obtaining binary rules to perform the final classification using a classification and regression tree (CART).

**Derivative Spectroscopy (DS)**: DS techniques have been extensively used to assess information regarding light absorption by significant water constituents [38,52–55]. As far as most differences in the visible range between macroalgae phyla are caused by absorption bands of their different pigments, spectral derivative analysis can be used to highlight absorption features [56–58], thus allowing quantification of "absorption troughs" [59]. DS points out differences in pigmentation and/or structural properties between targets [60,61], allowing macrophyte discrimination [54,62].

The objective of the present study is to compare the spectral separability capabilities of the three above described classification methodologies (RGB-colorimetry, TSS-OB and DS) introducing and using an extensive library with spectral signatures of 36 macroalgal species found in the eastern coast of the Atlantic Ocean.

## 2. Methodology

### 2.1. Algae library and study area

The study area where algae specimens were collected is located into the Ría de A Coruña, a small oceanic embayment (around 16 km$^2$) Northwest of Galicia (NW Spain). The Ría has a length of 5 km with a NS orientation in its main axis and a maximum width of 3 km at its mouth [63] (Fig. 1). This area contains rocky coasts with cliffs combined with sandy beaches having semi-diurnal tidal regime with a range of 3 m.

An extensive field campaign was carried out on 22nd and 23rd August 2009, in Praia de Canabal, a sandy beach 40 m long, placed in a small and protected bay located close to A Coruña city (Fig. 1, inset). For the collection of the present spectral library of macroalgae, samples of both wet algae floating near the water line and dried on the sand beach were measured on the shore nearby. Therefore, during this campaign every specimen found at different points along the beach (intertidal or subtidal) was sampled, including specimens in different health states, humidity conditions or state of growth. With the aim of generating a comprehensive spectral library, each gathered specimen was documented, photographed and its spectra measured immediately after collection to minimize water evaporation or specimen degradation by ambient temperature or handling. A total of 134 specimens from 36 different species were acquired: 16 brown, 17 red, and 3 green algae (see Table 2).

Spectral reflectance measurements were performed on the beach using a spectroradiometer (ASD FieldSpec Pro FR, Analytical Spectral Devices, Boulder, CO, US) with a spectral range of 350–2500 nm and a spectral sampling interval of 1.4 nm for the VNIR detector and 2.0 nm for the SWIR detector. Each specimen was illuminated with a continuous spectrum halogen lamp through a contact probe (ASD High Intensity Contact Probe, Analytical Spectral Devices, Boulder, CO, US). The specimens covered completely the contact probe window, that was held in tight contact to avoid specular reflections of the tissue-air interfaces (improving optical contact simulated the optical behavior of submerged samples), but not exerting much pressure that could affect the specimens vegetal structure. A fiber-optic cable, having a field of view of 25°, thus, spanning an area of several square centimeters of the specimen, transmitted the reflected light to the spectroradiometer (Fig. 2). A Spectralon® white reference was used to calibrate the reflectance spectra that were computed by the spectroradiometer control software. Ten measurements were performed of each specimen in order to compute spectral averages, thus reducing noise and discarding accidental measurement errors.

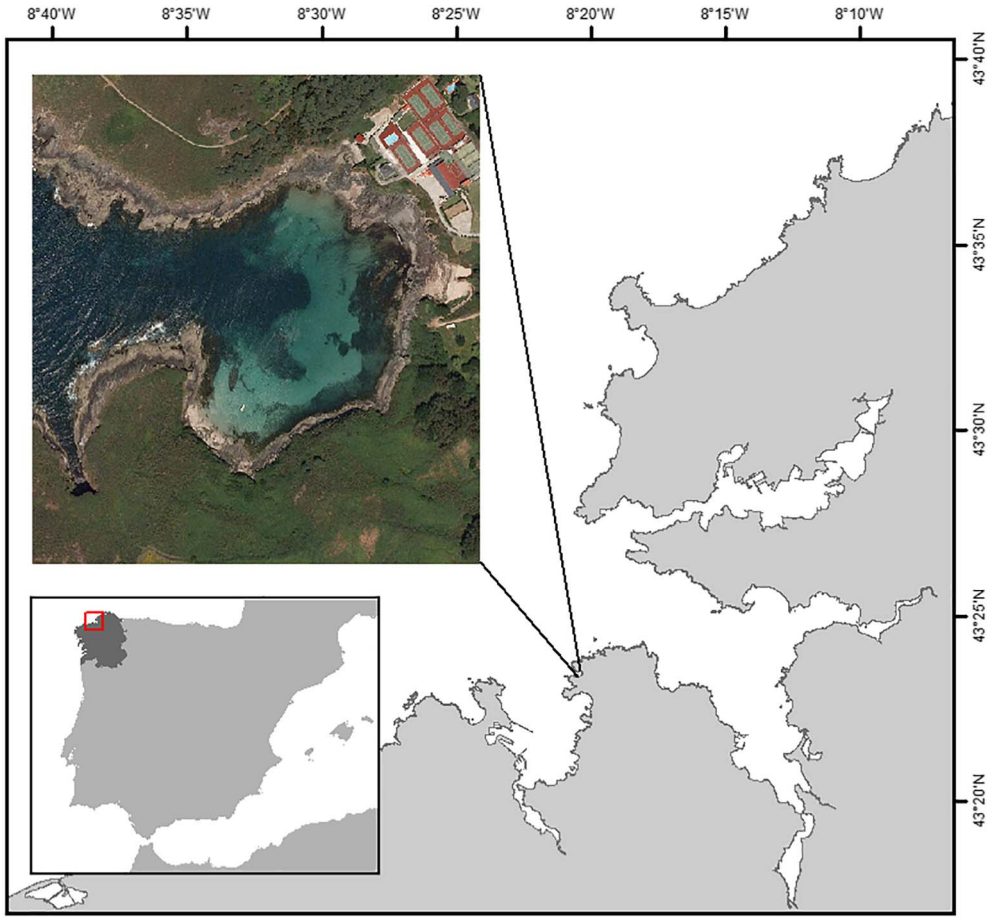


**Fig. 1.** Study area, Praia de Canabal in the Ria de A Coruña (Galicia, NW Spain).

**Table 2**
Algal species measured in the field campaign and their group classification.

| Brown algae | Green algae | Red algae |
|---|---|---|
| *Ascophyllum nodosum* | *Codium tomentosum* | *Asparagopsis armata* |
| *Bifurcaria bifurcata* | *Enteromorpha* sp. | *Bornetia secundiflora* |
| *Cladostephus spongiosus* | *Ulva* spp. | *Caulacanthus ustulatus* |
| *Colpomenia peregrina* | | *Ceramium rubrum* |
| *Cutleria multifida* | | *Chondracanthus acicularis* |
| *Cystoseira baccata* | | *Chondria dasyphylla* |
| *Cystoseira tamariscifolia* | | *Chondrus crispus* |
| *Dictyopteris polypodioides* | | *Corallina officinalis* |
| *Fucus spiralis* | | *Gelidium sesquipedale* |
| *Fucus vesiculosus* | | *Gigartina acicularis* |
| *Himanthalia elongata* | | *Gigartina piscillata* |
| *Laminaria saccharina* | | *Gigartina teedii* |
| *Phyllariopsis purpurascens* | | *Jania rubens* |
| *Sargassum muticum* | | *Laurencia obtusa* |
| *Stypocaulon scoparium* | | *Mastocarpus stellatus* |
| *Taonia atomaria* | | *Plocamium cartilagineum* |
| | | *Pterocladia capillacea* |


**Fig. 2.** Measuring the reflectance spectrum of one alga using the ASD-FR spectroradiometer.

### 2.2. Spectra processing and phyla separability

For every specimen, an averaged spectrum was computed from ten spectral reflectance measurements (each of them computed from an automatic average of 10 spectral radiance acquisitions). This had the effect of reducing electronic noise without losing spectral resolution (as a spectral smoothing filter would have caused).

The taxa separability of macroalgae has been addressed using the three different methods introduced above: RGB-colorimetry, TSS-OB and DS. The jackknife resampling technique [64] has been used to assess the accuracy of the RGB-colorimetry and TSS-OB methods by comparing each sample's known taxa with the classification performed training the algorithm with the remaining N − 1 measurements (N = 134), otherwise

independent. This training-classification-comparison is performed N times to assess the classification of each specimen from the rest of the set, thus simulating the chance of correctly classifying a newly acquired spectrum using the library trained algorithm.

#### 2.2.1. RGB-colorimetry

This methodology consisted in obtaining the standard RGB (sRGB) color coordinates from the averaged measured reflectance spectra of each specimen. The sRGB is computed in six steps: i) transform reflectance into standardized spectral radiance by multiplying by the CIE Standard Illuminant D65 [65]; ii) convert radiation spectra to color components scalarly multiplying by the three tristimulus functions for a 10° field of view $(\overline{x}, \overline{y}, \overline{z})$ (CIE 1991); iii) transform $(\overline{x}, \overline{y}, \overline{z})$ values into (r,g,b) primaries using a matrix transform based on the chromaticity coordinates and white reference of a standard computer monitor (ITU-R 2002) [49]; iv) crop to 0 the negative (r,g,b) primary values (RGB coordinates range from 0 to 1 and represent the fractional amount of each primary needed to display a particular color on a computer monitor); v) apply a gain factor of 20 (to provide more realistic colors resembling in situ photographs); vi) finally, apply a gamma transformation, with gamma equal to 2.4, to obtain the sRGB color coordinates (IEC 61966-2-1; [66]).

The sRGB color components are used to perform a linear classification of the three algae classes based on their sample colors. A logit model can be fitted using a generic linear model (GLM) assuming a binomial distribution to obtain the discriminant lines between green and brown algae, and brown and red ones. Considering a point in the plane of R-G color components, the mathematical problems to be optimized by the GLMs are given by:

$$\log \frac{P_{\text{red}}(R,G)}{P_{\text{brown}}(R,G)} = a_{\text{red}}R + b_{\text{red}}G + c_{\text{red}} \tag{1}$$

where $P_{\text{brown}} = 1 - P_{\text{red}} \sim$ binomial and the model is fitted with only the red and brown algae specimens, and

$$\log \frac{P_{\text{green}}(R,G)}{P_{\text{brown}}(R,G)} = a_{\text{green}}R + b_{\text{green}}G + c_{\text{green}} \tag{2}$$

where $P_{\text{brown}} = 1 - P_{\text{green}} \sim$ binomial, and the model is fitted with only the green and brown algae specimens. In both cases the right hand sides of equations, when equated to 0, represent the straight lines separating the two classes in the R-G color plane.

#### 2.2.2. True Skill Statistics Optimal Band (TSS-OB)

This approach was followed by Kotta et al. [37] and consists of two steps to compute the optimal boundary separation between phyla reflectances at each wavelength of the visible spectrum, between 400 and 700 nm: i) each specimen averaged spectrum was standardized (to 0 mean and 1 standard deviation) in the visible range by subtracting the mean and dividing by the standard deviation of the spectral reflectance in that band; ii) a threshold reflectance is computed such that each pair of phyla (red-green, red-brown and green-brown) is optimally separated by it, that is, for each wavelength in the interval 400–700 nm, most reflectances of specimens in one phylum lay above the threshold while most reflectances of specimens in the other phylum lay below. Mathematically expressed, $T_1$ is the fraction of "true results" above the threshold (i.e. reflectances of specimens belonging to the same phylum) and $T_2$ is the fraction of "true results" below, the sought for threshold must maximize the quantity

$$TSS = T_1 + T_2 - 1 \tag{3}$$

at a given wavelength. The threshold was found using an iterative method adapted from Kotta et al. [37].

#### 2.2.3. Derivative Spectroscopy (DS)

This approach consisted in locating the absorption maxima in the spectra and relating them with known absorption bands of algal photosynthetic pigments present in each phylum (Table 1): red algae are characterized by the presence of phycocyanin and phycoerythrin, pigments missing from brown and red algae; brown taxonomic group contains Chl-*c*, but not Chl-*b* and green algae have Chl-*b*, but not Chl-*c*. These characteristics provide a powerful method to discriminate macroalgae at phyla level. Absorption bands of these pigments are well-known [67–70] and are summarized in Table 3 as wavelength intervals.

**Table 3**
Absorption wavelength intervals of main pigments.

| Pigment | Wavelength range (nm) |
|---|---|
| Carotenes | 443–456 |
| Chl-*a* | 434–442, 667–685 |
| Chl-*b* | 468–478, 645–659 |
| Chl-*c* | 457–460, 582–596, 629–642 |
| Chl-*d* | 715–745 |
| Fucoxanthin | 489–491, 508–536 |
| Phycocyanin | 550–555, 608–628 |
| Phycoerythrin | 492–506, 537–549, 556–581, 597–605 |
| Zeaxanthin | 481–488 |

The absorption maxima were found from the zero crossings in the first order derivative of each spectrum, computed applying a digital Savitzky-Golay 3rd order filter, 15 nm in width [71]. Then the closest wavelength interval in Table 3 was chosen, with a tolerance of ± 7 nm, in order to determine pigments potentially present in each sample.

Finally, data analysis was performed over the 18 bands in Table 3 to find criterion for algae discrimination based on their presence, according to DS, in the specimen spectra. That criterion was formulated as a decision tree on the detection or not of those bands by DS, in particular bands of the phyla characteristic pigments: Chl-*b*, Chl-*c*, phycocyanin and phycoerythrin (see Fig. 8, below).

## 3. Results

The algae spectra included in this analysis form an extensive spectral library of Atlantic macroalgae: 134 specimens from 36 different species (see Annex A). They include not only species characteristics, but also intra-species phenological variability.

### 3.1. RGB-colorimetry

The sRGB color coordinates of each specimen were computed from its averaged reflectance spectrum (see Fig. 3 for examples of calculated sRGB and their matching with in situ photographs of the specimens). The resulting sRGB components were used to compute the linear classifiers for the three phyla. Each specimen was classified by training the algorithm without its own contribution, therefore classifiers differ from one another.

The resulting classification is shown in Fig. 4, which highlights that most of misclassified specimens are placed along the separation lines. The confusion matrix (Table 4a) for this classification shows that 83.3% of green, 63.6% of red, and 96.2% of brown algae specimens are correctly classified from their color (total accuracy, 84.3%). The Cohen's kappa coefficient (that takes into account the randomness effect caused by population sampling; [72]) was $\kappa = 0.697$, which stands for a good agreement.

A general classifier can be defined by calculating the averages of the 134 coefficients of linear boundaries given by fitting the logit models in Eqs. (1) and (2): $a_{\text{red}} = 18.30$, $b_{\text{red}} = 19.48$, $c_{\text{red}} = -3.59$; $a_{\text{green}} = -44.83$, $b_{\text{green}} = -36.12$, $c_{\text{green}} = 3.01$ (standard deviations are 0.42, 1.36, 0.24, 1.62, 1.15 and 0.29, respectively). Hence, the final linear classifier for the three phyla is:

Red algae: $G \leq 0.939R - 0.184$.
Brown algae: $0.939R - 0.184 < G < 1.241R - 0.073$

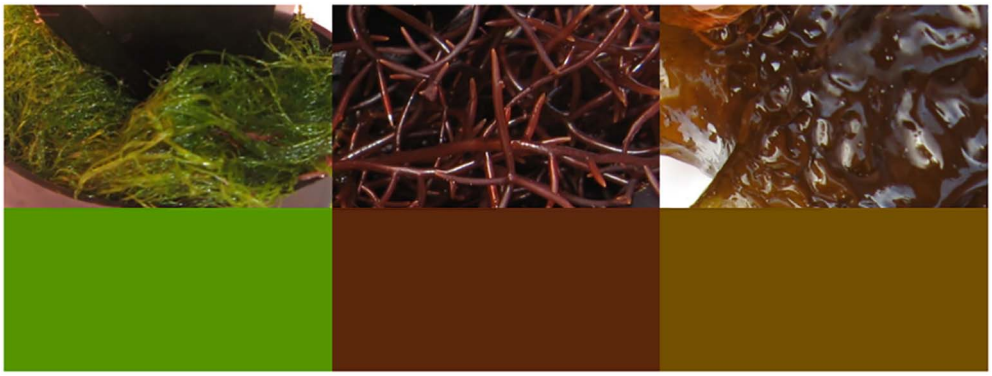

**Fig. 3.** Photographs of specimens taken during the field campaign compared with sRGB colors computed from their reflectance spectra.

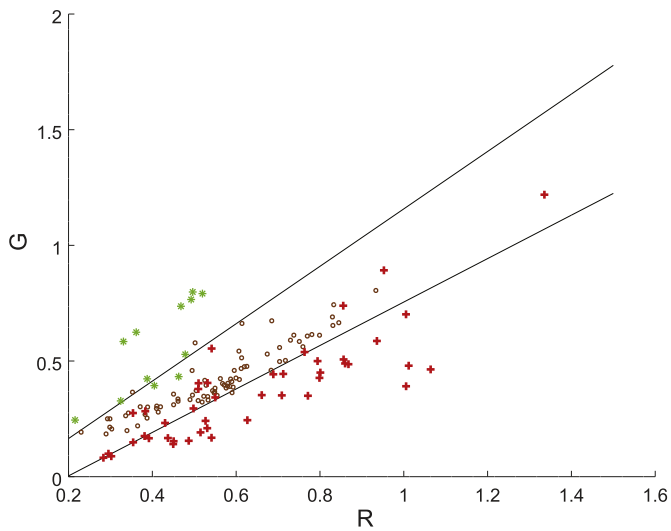


**Fig. 4.** Scatter plot of red (X axis) and green (Y axis) components of green (disks), red (crosses) and brown (circles) algae specimens, and their optimal linear classifiers, given by the straight lines $G = 0.939R - 0.184$ and $G = 1.241R - 0.073$.

**Table 4**
Confusion matrices of the three classifications (a: sRGB, b: TSS-OB and c: DS) of specimens in the spectral library.

| | Ground-truth | Spectral classification | | |
|---|---|---|---|---|
| | | Red | Green | Brown |
| *(a) RGB-colorimetry* | | | | |
| Red | 44 | 28 | 0 | 16 |
| Green | 12 | 0 | 10 | 2 |
| Brown | 78 | 1 | 2 | 75 |
| *(b) TSS-OB* | | | | |
| Red | 44 | 42 | 0 | 2 |
| Green | 12 | 0 | 11 | 1 |
| Brown | 78 | 4 | 1 | 73 |
| *(c) DS* | | | | |
| Red | 44 | 43 | 0 | 0 |
| Green | 12 | 0 | 11 | 0 |
| Brown | 78 | 2 | 0 | 73 |

Green algae: $G \geq 1.241R - 0.083$.

### 3.2. True Skill Statistics Optimal Band (TSS-OB)

The TSS decision rule provides a separation threshold at each wavelength for every pair of phyla, green-brown, red-brown, and green-red. Fig. 5 shows these thresholds (black points) besides the normalized spectra of each measured algae for every group. Every pair of phyla shows specific wavelengths in which the separation boundary is optimal (bold black points delimited by upright lines) (TSS over 0.95), these are separation bands in which spectra of two different phyla can be accurately discriminated (Fig. 5).

Based on these results, a classification of the major taxonomic groups can be performed using those optimal bands where TSS $>$ 0.95. Algorithm was trained 134 times, by removing one specimen at a time. The analysis of these data points shows the intervals from 590 to 609 nm, 621 to 660 nm, and 563 nm as the most suitable to separate green and red phyla. Green and brown phyla can be best discriminated in the ranges from 510 to 528 nm, 596 to 601 nm, and 646. Finally, red and brown phyla are more different in the interval from 643 to 656 nm.

These TSS criteria separate the measured spectra with high accuracy. According to the confusion matrix (Table 4b), 91.7% of green, 95.4% of red, and 93.4% of brown algae are correctly classified in their respective classes (total accuracy, 94.0%). The Cohen's kappa coefficient $\kappa = 0.891$, denotes a good agreement for this classification.

TSS-OB analysis generates a set of optimal bands where normalized reflectance thresholds do statistically separate the specimen spectra by phyla. In order to obtain bands more amenable to remote sensors, a hierarchical set of rules (or CART model) can be established (see Fig. 6). When tested against the entire spectral library, these ad hoc binary classification rules correctly assign 96.3% of the specimens (that would account for $\kappa = 0.933$; notice that these statistics are merely descriptive and not inferential as the ad hoc CART model has not been jackknifed).

### 3.3. Derivative Spectroscopy (DS)

Fig. 7 shows the first spectral derivatives in the visible region of one red, one green and one brown algae. Upward zero crossings of these spectra correspond to wavelengths of reflectance minima (i.e., absorption maxima) and they can be correlated with the pigment absorption wavelengths (Table 3). Zero crossing analysis is focused on the features associated with the three phyla pigments, Chl-*b*, Chl-*c*, phycoerythrin and phycocyanin, and results are summarized in Fig. 8 for all the specimens in the spectral library. It is apparent how the presence or absence of a few absorption bands characterizes most of the samples belonging to a class. The remaining absorption wavelengths of a given pigment although detectable in some species, often appear masked by other pigments, water absorption, frond structure, etc. Therefore, DS classification is performed based on a single absorption peak (wavelength of reflectance minimum) selected among those characterizing each pigment.

According to Fig. 8, most green algae have an absorption peak at 652 nm (Chl-*b*) that is missing in the brown algae. Additionally, absorption around 630–635 nm (Chl-*c*) is detected exclusively in brown algae. Moreover, red algae can be distinguished by the presence of phycoerythrin and phycocyanin absorbing at 492–499 nm and 615–630 nm, respectively. These results are consistent with the taxonomic features; brown macroalgae contain Chl-*c*, but not Chl-*b*; green ones have Chl-*b*, but not Chl-*c*; and red algae contain phycoerythrin and phycocyanin, missing in the others. Fig. 9 summarizes the classification

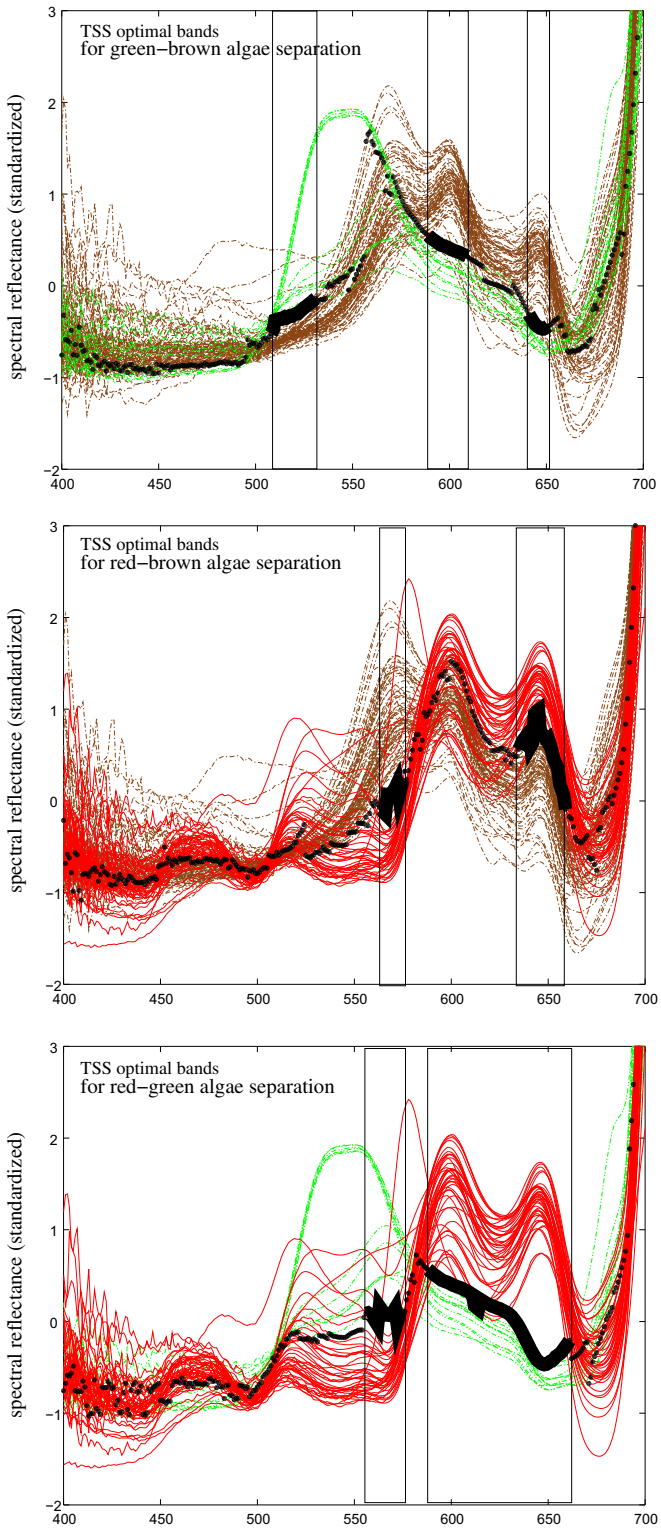


**Fig. 5.** Standardized spectra for each sample in the library (red, green and brown algae), and TSS boundaries in the visible range. Black lines highlight those boundaries with TSS > 0.95.

criteria derived from these observations, taking into account the wavelength intervals on Table 3.

The resulting DS classification groups sample spectra in phyla with a high accuracy. According to the confusion matrix (Table 4c), 91.7% of green, 97.7% of red, and 93.6% of brown algae are correctly classified (only 2 spectra appear misclassified, while another 5 are not classified at all; total accuracy, 94.8%). The Cohen's kappa coefficient, $\kappa = 0.910$, denotes a high agreement.

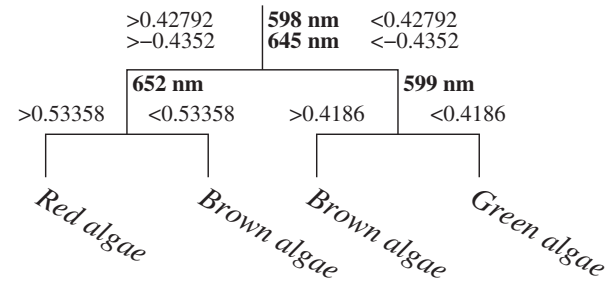


**Fig. 6.** Classification tree (wavelength (nm)–TSS boundaries) to separate major macroalgae groups.

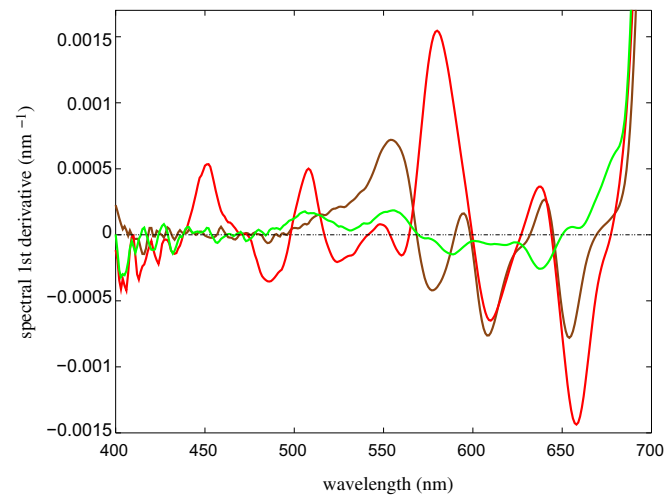


**Fig. 7.** First derivate spectra of a brown (*Ascophyllum nodosum*), a red (*Asparagopsis armata*), and a green (*Codium tomentosum*) alga in the visible range. Upward zero crossings correspond to wavelengths of reflectance minima and they can be correlated with pigments absorption.

## 4. Discussion

The goal of this study is to compare classification methods of macroalgae spectra. The in-air spectra measured can be seen as the best case scenario of the more general situation where algae may lay beneath a water column of any depth. The three approaches selected, RGB-colorimetry (sRGB), True Skill Statistics Optimal Band (TSS-OB) and Derivative Spectroscopy (DS) represent different technologies. In particular, sRGB would represent the human visual system (or a photographic camera), a rough type of three-band multispectral sensor as those found in hand-held cameras or true-color remote sensors. The TSS-OB would stand for a hyperspectral or an ad hoc multispectral sensor, the best case design possible for the purpose of algae classification. Finally, the DS would resemble a measure made with a hyperspectral sensor (on satellite or airborne).

All three methods provide a classification consistent with phyla determined in ground truth. This validation has been carried out using a comprehensive spectral library of key macroalgal species from the Atlantic Galician coast. Spectral libraries of macroalgae are scarce in the literature, and are mainly focused on the identification of average spectral signatures. This library complements and updates the libraries released to date [37,39–44] with its extensive catalog of 36 macroalgae species, many of them observed under different states of growth, health, humidity, etc. in order to enrich the library (see Annex A). The method validation is thus, the most extensive known to the authors ([37], includes 16 North Atlantic algal species; [44], includes 17 algal species from the Western Australian coast).

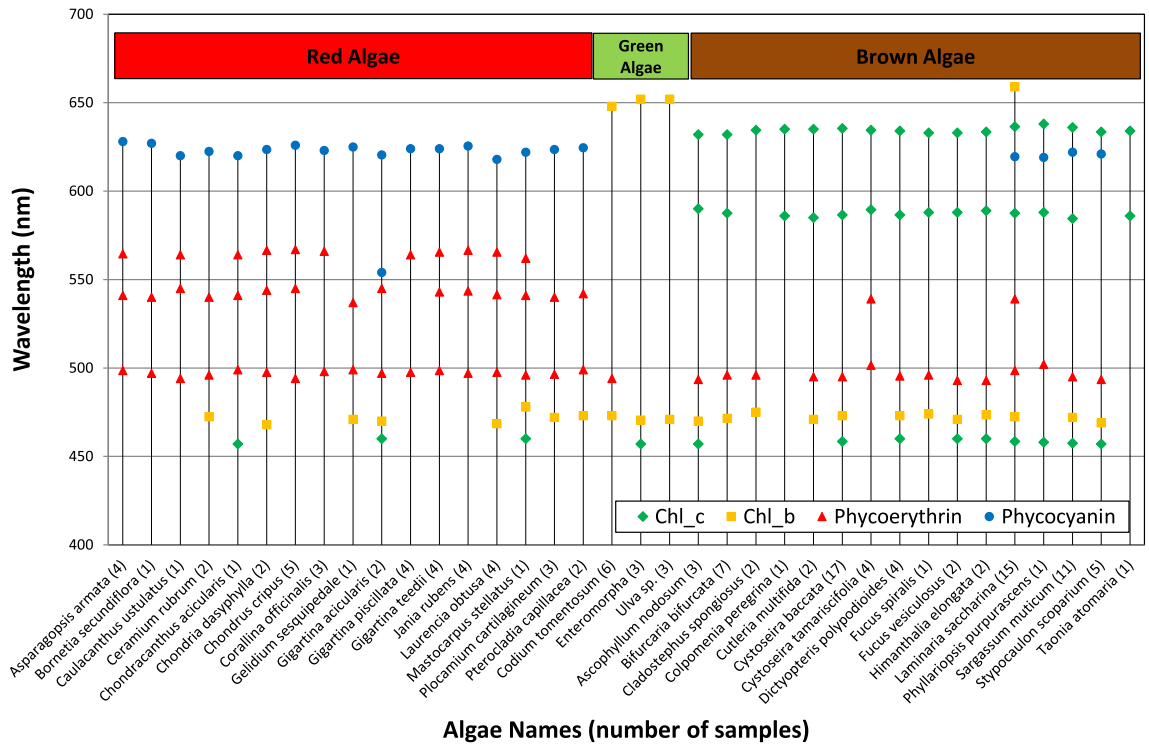


**Fig. 8.** Absorption wavelengths of most representative pigments of each phyla (Chl-*b* and Chl-*c*, phycoerythrin and phycocyanin), detected in the specimens of the spectral library. Numbers between parentheses denote the number of specimens studied of each species.

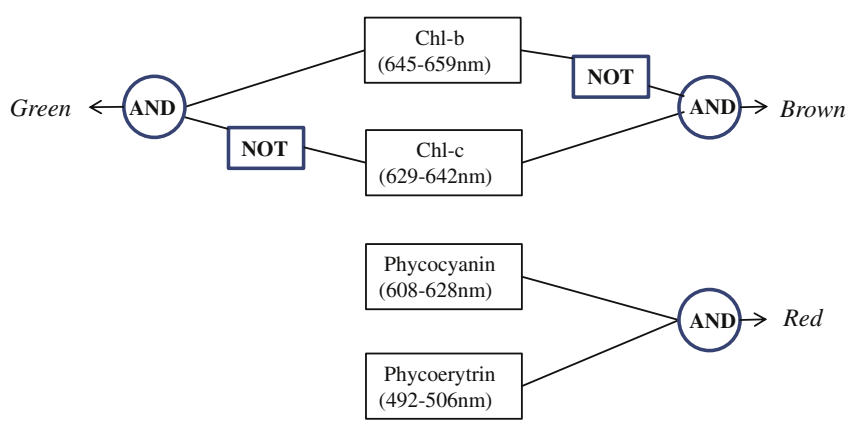


**Fig. 9.** Presence/absence criteria for pigment classification.

### 4.1. Resulting classifications

The sRGB-colorimetry shows that macroalgae groups at phyla level can be isolated with κ = 0.697, which is considered a good agreement with taxonomic classification. This approach, the weakest of all three (also the simplest one), misclassified 21 of the 134 measured spectra (corresponding to 15 different species) in phyla different from those determined during ground truthing. Many of them were misclassified because they lay very close to the separation lines in Fig. 3, where chromatic features from neighboring phyla coexist. Most misclassifications (17/21) appear between brown and red groups, something expected due to their chromatic similarities. Only 2 spectra of green algae *C. tomentosum* (the only green alga misclassified) were classified as brown, out of a total of 6, being the rest correctly classified as green; moreover the two misclassified spectra belonged to a group of 4 specimens washed away by the surge to the beach and thus the color is affected by the macroalgae health. Two spectra of brown algae, *L. saccharina* and *C. tamariscifolia*, were misclassified as green; *L. saccharina* spectrum corresponded to a dry specimen, meanwhile the *C. tamariscifolia* spectrum was the only misclassified one out of 4 from this species. It is noticeable that almost all species had at least one of their specimens correctly classified; only four species (*C. tamariscifolia*, *M. stellatus*, *C. ustulatus* and *C. acicularis*) had only one specimen measured, and *C. tamariscifolia* was partially mixed with other algae, according to the field notes. Other misclassifications are also associated with observations about partial dehydration of the samples taken on the beach.

Water content largely affects the visual aspect of a sample as it changes spectral reflectance along wide wavelength intervals. Taking this into account, it can be foretold that this method, based on human perception of color (i.e., on very wide spectral bands), must be the most sensitive to phenological state of the algae, and thus the less accurate. The other methods use either normalized spectral reflectance (TSS-OB), or spectral derivatives (DS), and, thus, are concerned with spectral features, not affected by enhanced light transmission through the tissues (that also enhances absorption by embedded pigments).

The TSS-OB approach shows a high agreement with phyla, κ = 0.891. The binary classification tree derived from TSS-OB (Fig. 6) shows that phyla separation is based on Chl-*b* (652 nm) and phycoer-

ythrin (599 nm) absorption bands, pigments characteristic of green and brown algae, respectively. In this sense no misclassification between both phyla is expected. However, the misclassification observed with sRGB method (brown algae classified as green) was observed here with the same spectrum of *C. tamariscifolia* (one of four spectra of this species) which suggests some anomaly in the specimen. Apart from this, the TSS-OB method only misclassified four brown macroalgae specimens: one *S. scoparium*, one *S. muticum*, one *B. bifurcata,* and one *L. saccharina* (all of them classified as red algae). In all these cases other spectra from these species were correctly classified.

The DS classification, which is based on pigment presence, provides the most accurate classification of macroalgae at phyla level, with $\kappa = 0.910$ (slightly above the TSS-OB). In this case, only 2 spectra, one specimen of *L. saccharina* and one of *S. muticum*, were misclassified (as red algae, instead of brown). Most significantly, the same misclassification of the *S. muticum* spectrum is found with the TSS-OB method. Furthermore, the same *L. saccharina* specimen, reference as dry in the field notes, is wrongly assigned by the sRGB approach that classifies it as green algae instead of brown. Finally, five spectra each belonging to *J. rubens*, *S. scoparium*, *L. saccharina*, *S. muticum* and *C. tomentosum* were not assigned to any phylum as we could not determine an exhaustive set of classification rules that covered all possibilities. Two of these spectra were misclassified by the previous methods, the red algae *J. rubens*, which was measured over its green part according to the field notes, is classified as brown by the sRGB, while the brown algae *S. scoparium* (one of the five specimens) is identified as red by TSS-OB.

The DS classification, as well as the TSS-OB, relays on Chl-*b* absorption at 652 nm to discriminate different phyla. Interestingly enough, in the case of phycoerythrin the selected absorption peak was different in both methods: TSS-OB chose the 598 nm peak, while DS detected more consistently the phycoerythrin band around 492–499 nm.

Misclassified spectra in all three methods are not always the same: only TSS-OB method shares misclassified spectra (*S. muticum*, *C. tamariscifolia*, *G. acicularis*, *G. piscillata* and *C. tomentosum*) with the other two. Misclassified or not-classified spectra in DS and sRGB methods are not related. In this sense, the measurement process does not explain all these discrepancies, although some influence cannot be discarded. A group of species that is difficult to classify (by any of the three methods) cannot be identified, as all species represented by more than one specimen have at least one spectrum correctly classified. Hence, misassignments seem related with different features triggered by same-species inter-specimen variations. It is known that pigment composition may vary not only between species of the same phylum but also between individuals of the same species due to different physiological state or environmental factors, such as light, nutrients and water flow [39,40,73], and this variability may hinder our spectral classifications.

### 4.2. Expected robustness of the results in real mapping situations

A current challenge for coastal researchers is relating the spectral response of aquatic vegetation to real mapping situations. Our study shows a minimalistic set of discriminant bands for each method showing the minimal requirements for its use as a remote sensing seagrass cartography tool: 2 wide bands for the sRGB, or 3 for the TSS-OB, or 4 narrow bands for the DS. The RGB-colorimetric approach can be used to classify algae laying on the beach or submerged in clear shallow waters using digital cameras or RGB sensors onboard unmanned aerial vehicles [74]. The bands determined by TSS-OB and DS are robust with respect to the phenological conditions of the algae included in the spectral library and may provide a criterion for selecting appropriate bands of remote sensors, or the most appropriate phylum classification method given those bands, e.g., using a hyperspectral camera [75].

Previous studies have considered the effect of water column on observed spectral reflectance. Vahtmäe et al. [41] measured reflectance spectra of green (*C. glomerata*), red (*F. lumbricalis*), and brown (*F. vesiculosus*) macroalgae and used a bio-optical model to predict that these algae can be optically distinguished from each other, or from sandy bottom or deep water in turbid water conditions. However, García et al. [44], also using a biooptical model, conclude that prior knowledge of the depth and optical properties of water are a prerequisite to perform a classification; i.e., effective differentiation of macroalgae depends not only on the species under consideration but also strongly on the water column. For instance, most wavelengths of features selected by our TSS-OB and DS methods fall above the 590 nm boundary where seawater absorption steeply increases with wavelength. Thus slight changes in depth will cause large changes in remotely sensed water leaving spectral reflectance well above that wavelength. Overlooking the effects water absorption may have on spectral normalization prior to TSS-OB, bands around 563 nm and 519 nm are suggested to differentiate between green-red and green-brown algae, respectively, as light is weakly absorbed in them. Similarly, DS method would detect red algae using the 495 nm phycoerythrin absorption band. However, only detection of very marked reflectance minima is guaranteed by the DS method at wavelengths between 580 nm and 610 nm, when specimens are submerged tens of centimeters below a clear water surface; fortunately, none of the DS characteristic absorption bands is found in this interval. The spectral library introduced in this work increases the opportunities of further studies assessing the effect of the water column (its depth and inherent optical properties) on the capabilities of remote sensors to achieve that differentiation.

### 4.3. Ecological implications/applications

As pointed out in the introduction, algal communities play a fundamental role in coastal region ecology. This is especially true for those forming forests whose spatio-temporal changes respond not only to natural [76] but also to anthropic activities, e.g. introduction of alien species [77], environmental pollution [78], and climate change [79]. Previous works have focused on monitoring the expansion of a single seaweed species, often brown macroalgae (e.g. [23,81]), or on the detection and quantification of blooms, such as green *Ulva* spp. (e.g. [82,83]).

What ecological use can be given to the spectral library and methods analyzed in this paper? Although ecological roles of macroalgae do not depend on their phylum, but on the functional structures of the species (i.e., thallus arrangement, shape, transparency, etc.; [80]), as a first approximation, identification of phylum differences may help in the assessment of ecosystem changes, e.g., in the case of an alien species invading a monospecies native forests (e.g. [84]).

Other uses can be found to the spectral library here introduced or to some partial results such as those in Fig. 8, which highlights the pigment absorption bands found in the specimens. Spectral analysis methodologies in remote sensing have addressed intraspecific differences in response to physiological [73,85] or seasonal changes [35]; however, this information can be useful to other researchers not limited to remote sensing.

## 5. Conclusions

In this work we have applied and compared three algae spectral classification methodologies: sRGB, TSS-OB and DS. The results have been obtained using an extensive spectral library including 36 macroalgal species of the East Atlantic Ocean, with different specimens of each species found in the study area in different conditions. Thus, the results obtained are quite robust to natural variability. From the results of the classifications, two principal conclusions can be drawn. The TSS-OB and the DS approaches provide almost perfect classifications (despite some anomalous specimens), being the DS better ($\kappa = 0.910$) requires fixed bands 10–20 nm in width, of the order of current hyperspectral remote sensors. TSS-OB ($\kappa = 0.891$) requires finer band selections as shown by the analysis. On the other hand, the sRGB approach, useful for in situ photographic classification, also provides good results ($\kappa = 0.697$), despite its much less demanding spectral bands. This work shows that algae phyla discrimination is possible using any of these methods

because spectral bands/features exist that minimize the effects of intra-species spectral variability caused by phenological or ambient conditions. However, the effect of the water column on the spectral reflectance should be taken into account in order to apply present results to clear or turbid deep waters and to get a joint understanding of the real macroalgae distribution over the NW Atlantic coastal area.

## Appendix A

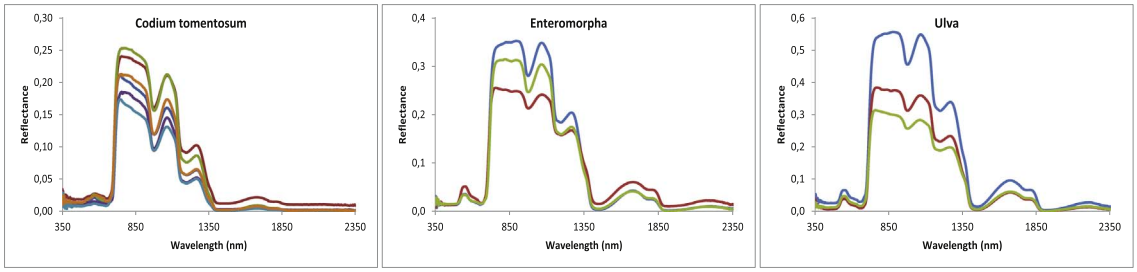


**Fig. A1.** Green alga spectra.

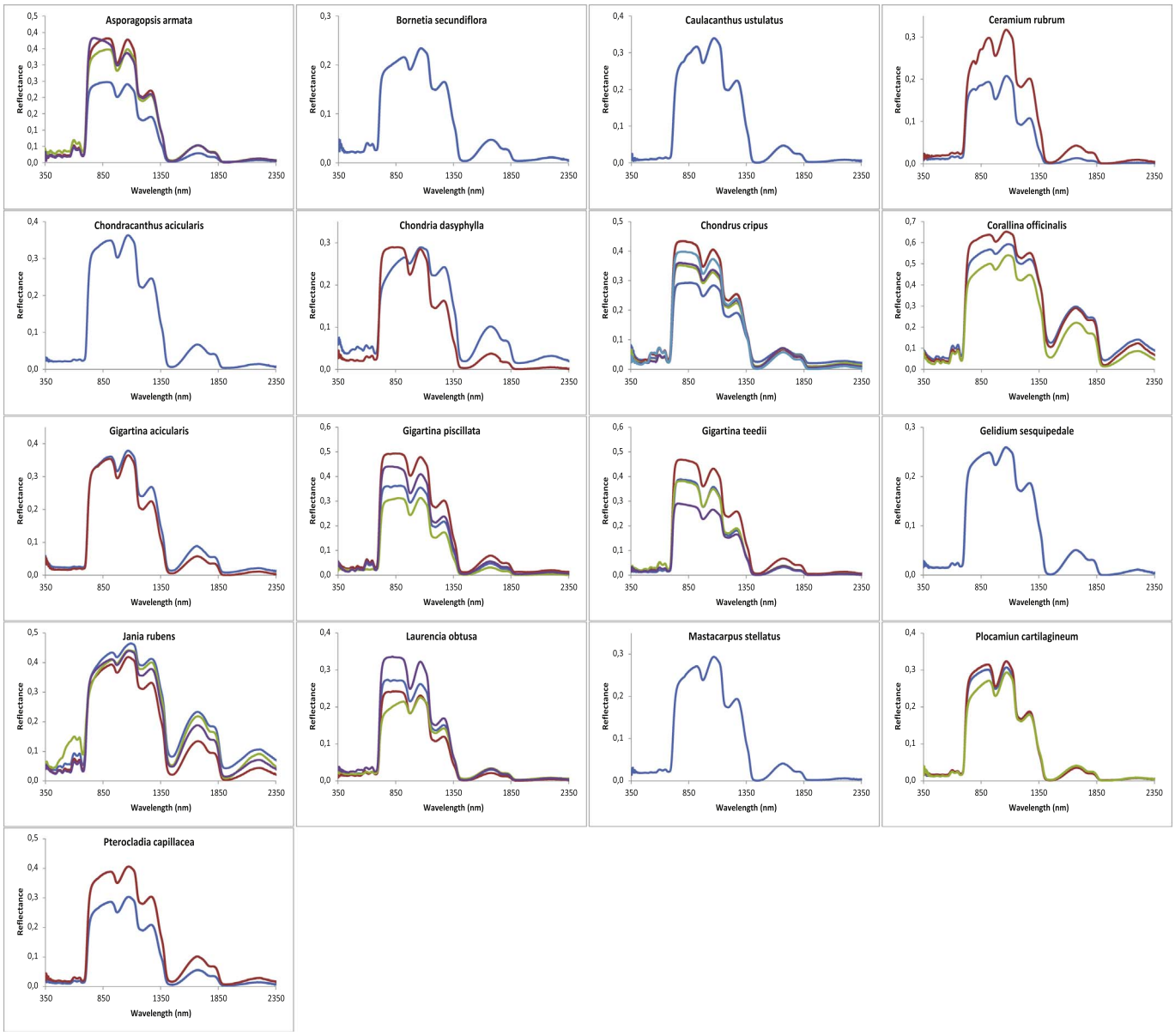


**Fig. A2.** Red algae spectra.

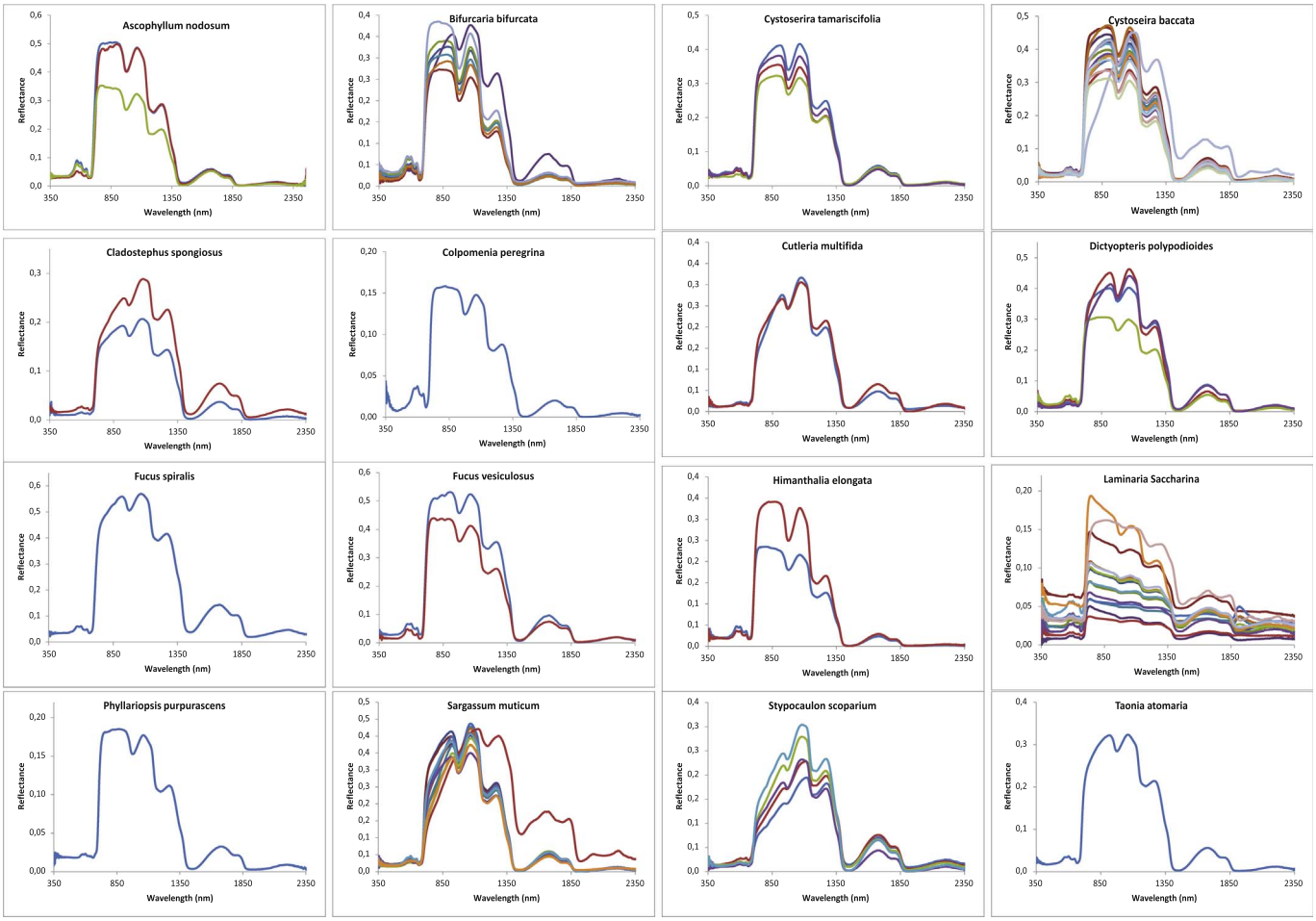


**Fig. A3.** Brown algae spectra.

## References

[1] D.A. Birkett, C.A. Maggs, M.J. Dring, P.J.S. Boaden, R. Seed, Infralittoral reef biotopes with kelp species. An overview of dynamic and sensitivity characteristics for conservation management of marine, SACs 7 (1998).

[2] A. Pallas, B. Garcia-Calvo, A. Corgos, C. Bernardez, J. Freire, Distribution and habitat use patterns of benthic decapod crustaceans in shallow waters: a comparative approach, Mar. Ecol. Prog. Ser. 324 (2006) 173–184.

[3] E. Cacabelos, A. Lourido, J.S. Troncoso, Composition and distribution of subtidal and intertidal crustacean assemblages in soft-bottoms of the Ria de Vigo (NW Spain), Sci. Mar. 74 (3) (2010) 455–464.

[4] Å. Borg, L. Pihl, H. Wennhage, Habitat choice by juvenile cod (*Gadus morhua* L.) on sandy soft bottoms with different vegetation types, Helgoländer Meeresun. 51 (2) (1997) 197–212.

[5] G.P. Shaffer, T.E. Perkins, S. Hoeppner, S. Howell, H. Benard, A.C. Parsons, Ecosystem health of the Maurepas Swamp: feasibility and projected benefits of a freshwater diversion, Final Report. US Environmental Protection Agency, Region, 2003, p. 6.

[6] A. Velando, J. Freire, Coloniabilidad y conservación de aves marinas: el caso del cormorán moñudo, Etología 7 (1999) 55–62.

[7] S.H. Lorentsen, D. Grémillet, G.H. Nymoen, Annual variation in diet of breeding great cormorants: does it reflect varying recruitment of gadoids? Waterbirds 27 (2) (2004) 161–169.

[8] A.H. Buschmann, Intertidal macroalgae as refuge and food for Amphipoda in central Chile, Aquat. Bot. 36 (3) (1990) 237–245.

[9] V. Gotceitas, S. Fraser, J.A. Brown, Use of eelgrass beds (*Zostera marina*) by juvenile Atlantic cod (*Gadus morhua*), Can. J. Fish. Aquat. Sci. 54 (6) (1997) 1306–1319.

[10] M.I. Abdullah, S. Fredriksen, Production, respiration and exudation of dissolved organic matter by the kelp *Laminaria hyperborea* along the west coast of Norway, J. Mar. Biol. Assoc. UK 84 (05) (2004) 887–894.

[11] A.J. Madsen, N.G. Plant, Intertidal beach slope predictions compared to field data, Mar. Geol. 173 (1) (2001) 121–139.

[12] J.-Y. Floc'h, R. Pajot, V. Mouret, *Undaria pinnatifida* (Laminariales, Phaeophyta) 12 years after its introduction into the Atlantic Ocean, Fifteenth International Seaweed Symposium, Springer Netherlands, 1996, pp. 217–222.

[13] R.M. Viejo, The effects of colonization by *Sargassum muticum* on tidepool macroalgal assemblages, J. Mar. Biol. Assoc. U. K. 77 (02) (1997) 325–340.

[14] J.R. Bidwell, K.W. Wheeler, T.R. Burridge, Toxicant effects on the zoospore stage of the marine macroalga *Ecklonia radiate* (Phaeophyta: Laminariales), Mar. Ecol. Prog. Ser. 163 (1998) 259–265.

[15] S.M. Coelho, J.W. Rijstenbil, M.T. Brown, Impacts of anthropogenic stresses on the early development stages of seaweeds, J. Aquat. Ecosyst. Stress. Recover. 7 (4) (2000) 317–333.

[16] K. Hiscock, A. Southward, I. Tittley, S. Hawkins, Effects of changing temperature on benthic marine life in Britain and Ireland, Aquat. Conserv. Mar. Freshwat. Ecosyst. 14 (4) (2004) 333–362.

[17] T. Vanderstraete, R. Goossens, T.K. Ghabour, Coral reef habitat mapping in the red sea (Hurghada, Egypt) based on remote sensing, EARSeL eProceedings 3 (2) (2004) 191–207.

[18] J.R. Jensen, J.E. Estes, L. Tinney, Remote-sensing techniques for kelp surveys, Photogramm. Eng. Remote. Sens. 46 (6) (1980) 743–755.

[19] E.W. Augenstein, D.A. Stow, A.S. Hope, Evaluation of SPOT HRV-XS data for kelp resource inventories, Photogramm. Eng. Remote. Sens. 57 (5) (1991) 501–509.

[20] T. Belsher, M.C. Mouchot, Use of satellite imagery in management of giant kelp resources, Morbihan Gulf, Kerguelen archipelago, Oceanol. Acta 15 (3) (1992) 297–307.

[21] S.R. Phinn, A.G. Dekker, V.E. Brando, C.M. Roelfsema, Mapping water quality and substrate cover in optically complex coastal and reef waters: an integrated approach, Mar. Pollut. Bull. 51 (1–4) (2005) 459–469.

[22] M.S. Stekoll, L.E. Deysher, M. Hess, A remote sensing approach to estimating harvestable kelp biomass, Eighteenth International Seaweed Symposium, Springer Netherlands, 2007, pp. 97–108.

[23] K.C. Cavanaugh, D.A. Siegel, B.P. Kinlan, D.C. Reed, Scaling giant kelp field measurements to regional scales using satellite observations, Mar. Ecol. Prog. Ser. 403 (1) (2010) 13–27.

[24] K.C. Cavanaugh, D.A. Siegel, D.C. Reed, P.E. Dennison, Environmental controls of giant-kelp biomass in the Santa Barbara Channel, California, Mar. Ecol. Prog. Ser. 429 (2011) 1–17.

[25] G. Casal, N. Sánchez-Carnero, E. Sánchez-Rodríguez, J. Freire, Remote sensing with SPOT-4 for mapping kelp forests in turbid waters on the south European Atlantic shelf, Estuar. Coast. Shelf Sci. 91 (3) (2011) 371–378.

[26] G. Casal, T. Kutser, J.A. Domínguez-Gómez, N. Sánchez-Carnero, J. Freire, Mapping

benthic macroalgal communities in the coastal zone using CHRIS-PROBA mode 2 images, Estuar. Coast. Shelf Sci. 94 (3) (2011) 281–290.
[27] E.J. Hochberg, M.J. Atkinson, Capabilities of remote sensors to classify coral, algae, and sand as pure and mixed spectra, Remote Sens. Environ. 85 (2003) 174–189.
[28] M. Reichstetter, P.R. Fearns, S.J. Weeks, L.I. McKinna, C. Roelfsema, M. Furnas, Bottom reflectance in ocean color satellite remote sensing for coral reef environments, Remote Sens. 7 (12) (2015) 16756–16777.
[29] A. Meinesz, Methods for identifying and tracking seaweed invasions, Bot. Mar. 50 (2007) 373–384.
[30] S. Katsanevakis, I. Wallentinus, A. Zenetos, E. Leppäkoski, M.E. Çinar, B. Oztürk, M. Grabowski, D. Golani, A.C. Cardoso, Impacts of invasive alien marine species on ecosystem services and biodiversity: a pan-European review, Aquat. Invasions 9 (4) (2014) 391–423.
[31] R.E. Lee, Phycology, Cambridge University Press, 2008.
[32] P.S. Dixon, Biology of the Rhodophyta, vol. 4, Oliver & Boyd, Edinburgh, 1973 (1973).
[33] G.M. Smith, Cryptogamic Botany: Algae and Fungi. Vol. I, MacGraw-Hill, New York, 1955.
[34] T. Kutser, A.G. Dekker, W. Skirving, Modeling spectral discrimination of Great Barrier Reef benthic communities by remote sensing instruments, Limnol. Oceanogr. Methods 48 (1) (2003) 497–510.
[35] T.W. Bell, K.C. Cavanaugh, D.A. Siegel, Remote monitoring of giant kelp biomass and physiological condition: an evaluation of the potential for the Hyperspectral Infrared Imager (HyspIRI) mission, Remote Sens. Environ. 167 (2015) 218–228.
[36] Z. Lee, K.L. Carder, C.D. Mobley, R.G. Steward, J.S. Patch, Hyperspectral remote sensing for shallow waters: deriving bottom depths and water properties by optimization, Appl. Opt. 38 (18) (1999) 3831–3843.
[37] J. Kotta, K. Remm, E. Vahtmäe, T. Kutser, H. Orav-Kotta, In-air spectral signatures of the Baltic Sea macrophytes and their statistical separability, J. Appl. Remote. Sens. 8 (1) (2014) 083634.
[38] J.D. Hedley, P.J. Mumby, Biological and remote sensing perspectives of pigmentation in coral reef organisms, Adv. Mar. Biol. 43 (2002) 277–317.
[39] T. Kutser, E. Vahtmäe, L. Metsamaa, Spectral library of macroalgae and benthic substrates in Estonian coastal waters, Proc. Est. Acad. Sci. Biol. Ecol. 55 (4) (2006) 329–340.
[40] T. Kutser, E. Vahtmäe, G. Martin, Assessing suitability of multispectral satellites for mapping benthic macroalgal cover in turbid coastal waters by means of model simulations, Estuar. Coast. Shelf Sci. 67 (3) (2006) 521–529.
[41] E. Vahtmäe, T. Kutser, G. Martin, J. Kotta, Feasibility of hyperspectral remote sensing for mapping benthic macroalgal cover in turbid coastal waters—a Baltic Sea case study, Remote Sens. Environ. 101 (3) (2006) 342–351.
[42] A. Thorhaug, A.D. Richardson, G.P. Berlyn, Spectral reflectance of the seagrasses: *Thalassia testudinum*, *Halodule wrightii*, *Syringodium filiforme* and five marine algae, Int. J. Remote Sens. 28 (7) (2007) 1487–1501.
[43] R. Pu, S. Bell, L. Baggett, C. Meyer, Y. Zhao, Discrimination of seagrass species and cover classes with in situ hyperspectral data, J. Coast. Res. 28 (6) (2012) 1330–1344.
[44] R.A. García, J.D. Hedley, H.C. Tin, P.R.C.S. Fearns, A method to analyze the potential of optical remote sensing for benthic habitat mapping, Remote Sens. 7 (10) (2015) 13157–13189.
[45] G. Casal, N. Sánchez-Carnero, J.A. Domínguez-Gómez, T. Kutser, J. Freire, Assessment of AHS (Airborne Hyperspectral Scanner) sensor to map macroalgal communities on the Ría de Vigo and Ría de Aldán coast (NW Spain), Mar. Biol. 159 (9) (2012) 1997–2013.
[46] G. Casal, T. Kutser, J.A. Domínguez-Gómez, N. Sánchez-Carnero, J. Freire, Assessment of the hyperspectral sensor CASI-2 for macroalgal discrimination on the Ría de Vigo coast (NW Spain) using field spectroscopy and modelled spectral libraries, Cont. Shelf Res. 55 (2013) 129–140.
[47] E. Vahtmäe, T. Kutser, Classifying the Baltic Sea shallow water habitats using image-based and spectral library methods, Remote Sens. 5 (2013) 2451–247447.
[48] S. Novoa, M. Wernand, H.J. van der Woerd, WACODI: a generic algorithm to derive the intrinsic color of natural waters from digital images, Limnol. Oceanogr. Methods 13 (12) (2015) 697–711.
[49] H.M. Dierssen, R.M. Kudela, J.P. Ryan, R.C. Zimmerman, Red and black tides: quantitative analysis of water-leaving radiance and perceived color for phytoplankton, colored dissolved organic matter, and suspended sediments, Limnol. Oceanogr. 51 (6) (2006) 2646–2690.
[50] G. Winters, R. Holzman, A. Blekhman, S. Beer, Y. Loya, Photographic assessment of coral chlorophyll contents: implications for ecophysiological studies and coral monitoring, J. Exp. Mar. Biol. Ecol. 380 (1) (2009) 25–35.
[51] O. Allouche, A. Tsoar, R. Kadmon, Assessing the accuracy of species distribution models: prevalence, kappa and the true skill statistic (TSS), J. Appl. Ecol. 43 (6) (2006) 1223–1232.
[52] R.J. Murphy, T.J. Tolhurst, M.G. Chapman, A.J. Underwood, Estimation of surface chlorophyll-a on an emersed mudflat using field spectrometry: accuracy of ratios and derivative-based approaches, Int. J. Remote Sens. 26 (9) (2005) 1835–1859.
[53] E. Torrecilla, J. Piera, M. Vilaseca, Derivative analysis of hyperspectral oceanographic data, in: G. Jedlovec (Ed.), Advances in Geoscience and Remote Sensing, InTech Open Access Publisher, 2009(ISBN: 978-953-307-005-6).
[54] F. Uhl, N. Oppelt, I. Bartsch, Spectral mixture of intertidal marine macroalgae around the island of Helgoland (Germany, North Sea), Aquat. Bot. 111 (2013) 112–124.
[55] C. Hu, L. Feng, R.F. Hardy, E.J. Hochberg, Spectral and spatial requirements of remote measurements of pelagic *Sargassum* macroalgae, Remote Sens. Environ. 167 (2015) 229–246.
[56] W.T. Butler, D.W. Hopkins, Higher derivative analysis of complex absorption spectra, Photochem. Photobiol. 12 (6) (1970) 439–450.
[57] T.H. Demetriades-Shah, M.D. Steven, J.A. Clark, High resolution derivative spectra in remote sensing, Remote Sens. Environ. 33 (1) (1990) 55–64.
[58] D.C. Rundquist, L. Han, J.F. Schalles, J.S. Peake, Remote measurement of algal chlorophyll in surface waters: the case for the first derivative of reflectance near 690 nm, Photogramm. Eng. Remote. Sens. 62 (2) (1996) 195–200.
[59] K.E. Joyce, S.R. Phinn, Hyperspectral analysis of chlorophyll content and photosynthetic capacity of coral reef substrates, Limnol. Oceanogr. 48 (1 Part 2) (2003) 489–496.
[60] P.J. Curran, J.L. Dungan, B.A. Macler, S.E. Plummer, The effect of a red leaf pigment on the relationship between red edge and chlorophyll concentration, Remote Sens. Environ. 35 (1) (1991) 69–76.
[61] G.A. Blackburn, Quantifying chlorophylls and caroteniods at leaf and canopy scales: an evaluation of some hyperspectral approaches, Remote Sens. Environ. 66 (3) (1998) 273–285.
[62] N. Oppelt, F. Schulze, I. Bartsch, K. Doernhoefer, I. Eisenhardt, Hyperspectral classification approaches for intertidal macroalgae habitat mapping: a case study in Heligoland, Opt. Eng. 51 (11) (2012) 111703-1.
[63] M. Varela, R. Prego, M. Canle, J. Lorenzo, The Ria de La Coruña, is hydrologically a ria, Gaia 9 (1994) 3–5.
[64] J.W. Tukey, Bias and confidence in not-quite large samples (abstract), Ann. Math. Stat. 29 (1958) 614.
[65] O. Noboru, A.R. Robertson, 3.9: standard and supplementary illuminants, Colorimetry, Wiley, 2005, pp. 92–96.
[66] C.A. Poynton, Digital Video and HDTV: Algorithms and Interfaces, Morgan Kaufmann, 2003 (ISBN 1-55860-792-7).
[67] V. Méléder, L. Barillé, P. Launeau, V. Carrère, Y. Rincé, Spectrometric constraint in analysis of benthic diatom biomass using monospecific cultures, Remote Sens. Environ. 88 (4) (2003) 386–400.
[68] L.G. Kwa, Study of Protein-Bacteriochlorophyll and Protein-Lipid Interactions of Natural and Model Light-harvesting Complex 2 in Purple Bacterium *Rhodobacter sphaeroides*, LMU, 2007 (Doctoral dissertation).
[69] K.H. Szekielda, J.H. Bowles, D.B. Gillis, W.D. Miller, Interpretation of absorption bands in airborne hyperspectral radiance data, Sensors 9 (4) (2009) 2907–2925.
[70] C. Hubas, B. Jesus, C. Passarelli, C. Jeanthon, Tools providing new insight into coastal anoxygenic purple bacterial mats: review and perspectives, Res. Microbiol. 162 (9) (2011) 858–868.
[71] C. Ruffin, R.L. King, The analysis of hyperspectral data using Savitzky-Golay filtering-theoretical basis (part 1), Geoscience and Remote Sensing Symposium, 1999, IGARSS'99 Proceedings. IEEE 1999 International, vol. 2, IEEE, 1999(1999).
[72] J. Cohen, A coefficient of agreement for nominal scales, Educ. Psychol. Meas. 2 (1960) 37–46.
[73] S.K. Fyfe, Spatial and temporal variation in spectral reflectance: are seagrass species spectrally distinct? Limnol. Oceanogr. 48 (1 Part 2) (2003) 464–479.
[74] K.F. Flynn, S.C. Chapra, Remote sensing of submerged aquatic vegetation in a shallow non-turbid river using an unmanned aerial vehicle, Remote Sens. 6 (12) (2014) 12815–12836.
[75] D. van der Wal, J. van Dalen, A. Wielemaker-van den Dool, J.T. Dijkstra, T. Ysebaert, Biophysical control of intertidal benthic macroalgae revealed by high-frequency multispectral camera images, J. Sea Res. 90 (2014) 111–120.
[76] Buschmann, A.H., Moreno, C., Vasquez, J.A. Hernández-Gonzalez, M.C. (2007). Reproduction strategies of *Macrocystis pyrifera* (Phaeophyta) in Southern Chile: the importance of population dynamics. Proceedings of the Eighteenth International Seaweed Symposium. R. Anderson, J. Brodie, E. Onsoyen A.T. Critchley, Springer Netherlands, 2007.
[77] E. Cacabelos, C. Olabarria, R.M. Viejo, M. Rubal, P. Veiga, M. Incera, I. Gestoso, F. Vaz-Pinto, A. Mejia, A.H. Engelen, F. Arenas, Invasion of *Sargassum muticum* in intertidal rockpools: patterns along the Atlantic Iberian Peninsula, Mar. Environ. Res. 90 (2013) 18–26.
[78] R.F. Piola, E.L. Johnston, Pollution reduces native diversity and increases invader dominance in marine hard-substrate communities, Divers. Distrib. 14 (2) (2008) 329–342.
[79] L. Duarte, R.M. Viejo, B. Martinez, M. de Castro, M. Gomez-Gesteira, T. Gallardo, Recent and historical range shifts of two canopy-forming seaweeds in North Spain and the link with trends in sea surface temperature, Acta Oecol. 51 (2013) 1–10.
[80] Hay, M.E. (1986). Functional geometry of seaweeds: ecological consequences of thallus layering and shape in contrasting light environments. On the Economy of Plant Form and Function, T.J. Givnish, Cambridge University Press, 1986.
[81] A.H. Buschmann, S.V. Pereda, D.A. Varela, J. Rodríguez-Maulén, A. López, L. González-Carvajal, ... M.C. Hernández-González, Ecophysiological plasticity of annual populations of giant kelp (*Macrocystis pyrifera*) in a seasonally variable coastal environment in the Northern Patagonian Inner Seas of Southern Chile, J. Appl. Phycol. 26 (2) (2014) 837–847.
[82] C. Hu, D. Li, C. Chen, J. Ge, F.E. Muller-Karger, J. Liu, F. Yu, M.-X. He, On the recurrent *Ulva prolifera* blooms in the Yellow Sea and East China Sea, J. Geophys. Res. 115 (2010) C05017.
[83] Q. Xu, H. Zhang, L. Ju, M. Chen, Interannual variability of *Ulva prolifera* blooms in the Yellow Sea, Int. J. Remote Sens. 35 (11 − 12) (2014) 4099–4113.
[84] R.E. Scheibling, P. Gagnon, Competitive interactions between the invasive green alga *Codium fragile* ssp. *tomentosoides* and native canopy-forming seaweeds in Nova Scotia (Canada), Mar. Ecol. Prog. Ser. 325 (2006) 1–14.
[85] H.M. Dierssen, A. Chlus, B. Russell, Hyperspectral discrimination of floating mats of seagrass wrack and the macroalgae *Sargassum* in coastal waters of Greater Florida Bay using air-borne remote sensing, Remote Sens. Environ. 167 (2015) 247–258.